



### 3.2 Wake Vortex Scenarios Simulation Package for Take-Off and Departure

Frank Holzäpfel<sup>1</sup>, Jan Kladetzke<sup>2</sup>

<sup>1</sup>*Institute of Atmospheric Physics*, <sup>2</sup>*Institute of Robotics and Mechatronics*

The WakeScene-D software package (Wake Vortex Scenarios Simulation Package for Departure) has been developed for comprehensive airspace simulations of take-off and departure. WakeScene-D consists of modules that model traffic mix, aircraft trajectories, meteorological conditions, wake vortex evolution, and potential hazard area. The software package estimates the probability to encounter wake vortices in different traffic and crosswind scenarios using Monte Carlo simulation in a domain ranging from the runway to an altitude of 3000 ft above ground. A comparison to measured vortex tracks of about 10,000 departures from runway 25R of Frankfurt airport indicates good agreement of global wake vortex transport characteristics in ground proximity. The standard departure situation employing a two-minute aircraft separation is compared to scenarios with reduced departure separations and various crosswind conditions. Comprehensive sensitivity analyses have been conducted which are briefly recapitulated. Effects related to departure route combinations and wind direction sectors are reported in more detail. Finally, an advanced scenario with an asymmetric crosswind criterion is introduced.

#### Introduction

Aircraft generated wake vortices pose a potential risk to following aircraft in various flight phases, whereas most wake vortex encounters are reported for approach and landing and for take-off and climb (Elsenaar et al. 2006). The ICAO wake-vortex aircraft separation standards (ICAO 2001) established in the 70's increasingly degrade aviation efficiency when traffic congestion limits airport capacity during landing and take-off. Research has shown that the transport and persistence of wake vortices are highly dependent on meteorological conditions (Gerz et al. 2005, Hallock et al. 1998), so that in many cases the separation standards are over-conservative. For single-runway operations, analyses (de Bruin et al. 2003, Frech & Zinner 2004, Frech & Holzäpfel 2008) suggest that, above a certain crosswind threshold, vortices are blown out of the flight corridor and pose no further threat to following aircraft.

The EU-project CREDOS (Crosswind-Reduced Separations for Departure Operations, see [www.euro-control.int/eec/credos/](http://www.euro-control.int/eec/credos/)) intends to demonstrate the operational feasibility of a concept of operations that uses measures of the prevailing crosswind component to allow temporary suspension of the need to apply wake vortex separations between successive departing aircraft. The focus on the combination of crosswind and departures has significant advantages: The follower aircraft is still on the ground when the controller schedules the separation. So the controller always has the possibility to extend the separation without requiring the pilot to make a maneuver. This beneficial situation also reduces the time horizon for which crosswind conditions must be anticipated. Secondly, in contrast to arrival situations the leader aircraft is generally faster so that the actual separations tend to increase.

WakeScene-D (Wake Vortex Scenarios Simulation Package for Departure) (Holzäpfel et al. 2009-2, Holzäpfel & Kladetzke 2011) is an extension of WakeScene which has been developed for approach and landing and is described in detail in (Holzäpfel et al. 2009-1). WakeScene-D estimates the probability to encounter wake vortices in different traffic and crosswind scenarios using Monte Carlo simulation in a domain ranging from the runway to an altitude of 3000 ft above ground. In cases with potential wake encounters all relevant parameters can be provided to VESA (Vortex Encounter Severity Assessment, Höhne et al. 2004, Luckner et al. 2004, Kauertz et al. 2012), a tool developed by Airbus, which may subsequently perform detailed investigations of the severity of the encounter. WakeScene-D consists of elements that model traffic mix, aircraft trajectories, meteorological conditions, wake vortex evolution, and potential hazard area. The process and data flows are controlled and evaluated by the MATLAB-based environment MOPS (Multi Objective Parameter Synthesis, Joos et al. 2002). Within CREDOS

WakeScene-D is used to support the definition of suitable crosswind criteria that allow reducing aircraft separations, to identify the sensitivity and interplay of the employed sub-models and parameter combinations, and to support risk analyses taking into account a broad range of variables which determine the probability and risk of a wake vortex encounter.

Related models have been developed for approach and landing: (1) WAVIR (Wake Vortex Induced Risk, Speijker et al. 2000) which is capable to estimate frequencies of certain risk events in a given scenario. (2) ASAT (Airspace Simulation and Analysis for TERPS where TERPS stands for Terminal Instrument Procedures) is a multifaceted computer tool for aviation related simulations and safety evaluations which has not been specifically designed as a wake vortex risk assessment model. Similar to WakeScene, ASAT has an interface to VESA that permits subsequent wake vortex encounter severity assessment. (3) The Vortex Risk Analysis Tool has been employed for the risk assessment of the High Approach Landing System / Dual Threshold Operation (HALS/DTOP) implemented at Frankfurt airport. HALS/DTOP aims at increasing the capacity of the closely spaced parallel runway system by employing a second threshold displaced by 1500 meters for the southern runway. (4) A comprehensive air traffic control wake vortex safety and capacity integrated platform has also been generated in the EU project ATC-Wake (Speijker et al. 2007). Elsenaar et al. (2006) provides a comprehensive survey on operational concepts designated to increase airport capacity and the regulatory framework which is relevant for the associated risk assessments as well as many other wake vortex related issues.

First, this paper describes the operating sequence of WakeScene-D and the employed sub-models. Next, a reference scenario is introduced which shall represent the real current departure situation. Then the statistics achieved with reduced aircraft departure separations and different crosswind thresholds are discussed. The paper highlights a selection of the most interesting results found in the conducted comprehensive sensitivity analyses. The investigated parameters of these sensitivity analyses comprise effects related to different departure route combinations, variations of flight path adherence, different wake vortex models, the development of aircraft separations during the departures, the sample size of the Monte Carlo simulations, aircraft type combinations, aircraft take-off weights, meteorological conditions, and airport operation times. Vortex tracks of about 10,000 departures collected during a six-month measurement campaign at Frankfurt airport are compared to WakeScene-D simulations and a comparison of the arrival and departure situation is conducted. On one hand, the sensitivity analyses help to increase the confidence in the software package and, on the other hand, they allow identifying the parameters that control encounter probabilities during takeoff and departure. In a next step the knowledge of these key parameters enables the optimization of criteria for reduced aircraft separations under favorable crosswind conditions. The current report is based on Holzäpfel et al. (2009) and Holzäpfel & Kladetzke (2011); a more detailed description of the sensitivity analysis is available in Holzäpfel & Kladetzke (2009).

### **Survey on Operating Sequence**

The flowchart depicted in Figure 1 sketches the operating sequence of WakeScene-D. Via simulation control (MOPS) the types of the generator aircraft and follower aircraft, the departure routes (see Figure 2), and a number of aircraft and pilot parameters are selected. The Trajectory Model provides time, speed, position, attitude, lift and mass of generator and follower aircraft along the flight paths.

Wake vortex evolution is predicted within control gates which are released along the flight path of the wake vortex generator aircraft in predefined time increments of e.g. 5 s. The gates' orientations are perpendicular to the aircraft true heading and perpendicular to the flight path angle (see Figure 3). Based on vertical profiles of wind speed and direction, air density, virtual potential temperature, turbulent kinetic energy, and eddy dissipation rate (Meteorological Data Base) and aircraft position, speed, attitude, lift, and span (Trajectory Model) at one gate, the Wake Vortex Model simulates the development of wake vortex trajectories, circulation, vortex core radius, and attitude of wake vortex axes. The Simplified Hazard Area Prediction model (SHAPE) computes the distance between wake vortex and follower aircraft



within each gate and discriminates between potentially critical cases and cases where safe and undisturbed flight is guaranteed. From all these data MOPS computes defined criteria, like minimal distance between wake vortex and follower aircraft and the respective vortex circulation and height, which are interpolated between the gates and statistically analysed. Finally, data needed for further investigations with VESA are deduced and stored. The results are optionally visualised in graphs of the statistics, 2D and 3D views (see Figure 3) or animations of the approaches of subsequent aircraft.

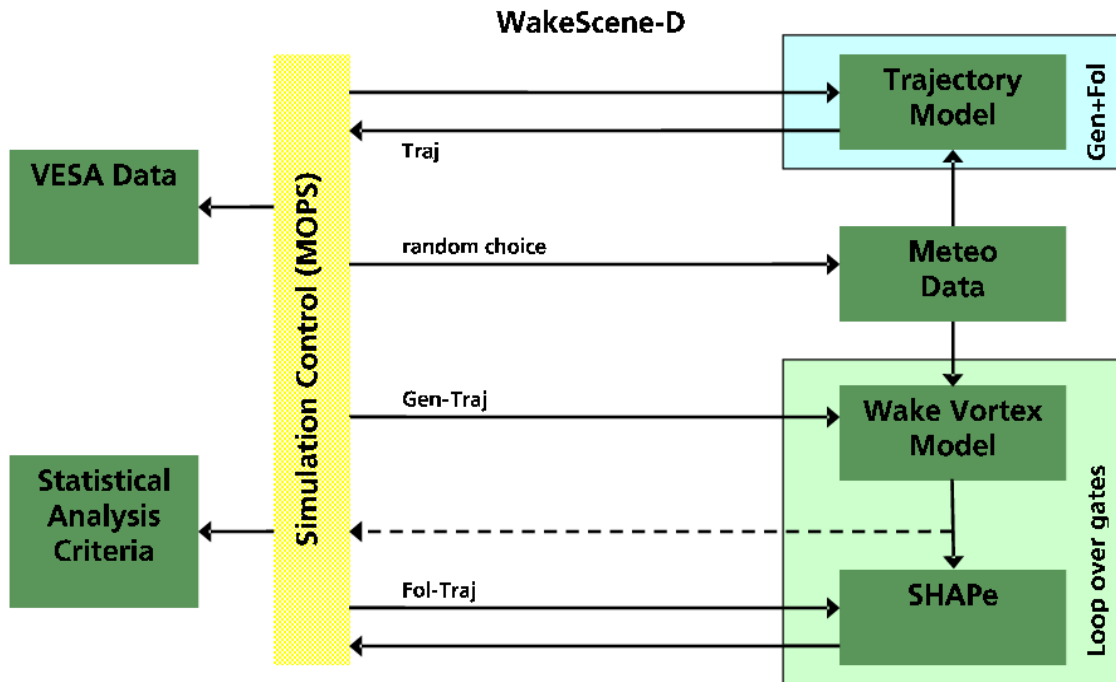


Figure 1. WakeScene-D flowchart. Arrows denote the data flow.

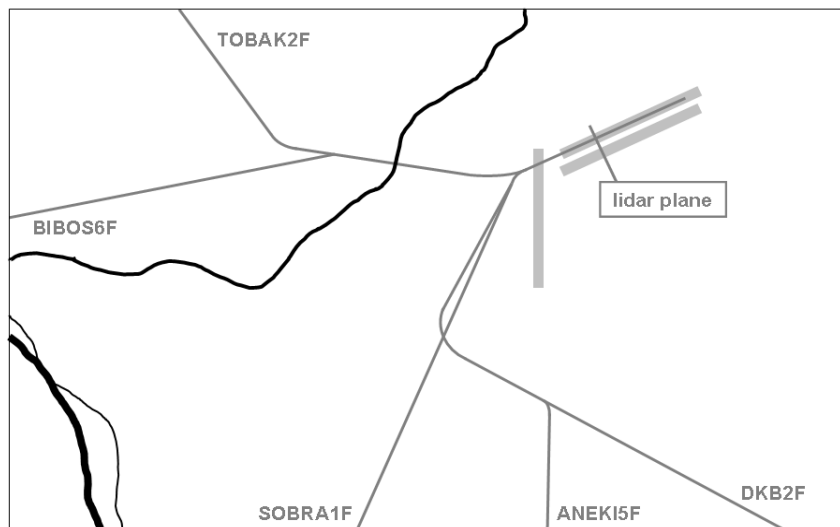


Figure 2. Runways, standard instrument departure routes (SIDS), and lidar measurement plane.

### Employed Models and Data Bases

The sub-models and data bases which are employed by WakeScene-D are briefly introduced in the subsequent paragraphs followed by a brief estimation of the related uncertainties.

### Meteorological Data Base

The variety of parameter combinations observed in the planetary boundary layer and their transformation on wake vortex behavior lead to a significant manifold of situations. To capture this diversity an extensive one-year simulation of realistic meteorological conditions has been produced for the Frankfurt terminal area with the non-hydrostatic mesoscale weather forecast model system NOWVIV (NOWcasting Wake Vortex Impact Variables, Gerz et al. 2005). NOWVIV comprises a full physics package including boundary layer turbulence, surface energy and momentum balance, soil physics, radiation processes including cloud effects, cumulus convection, and cloud physics (Grell et al. 2000).

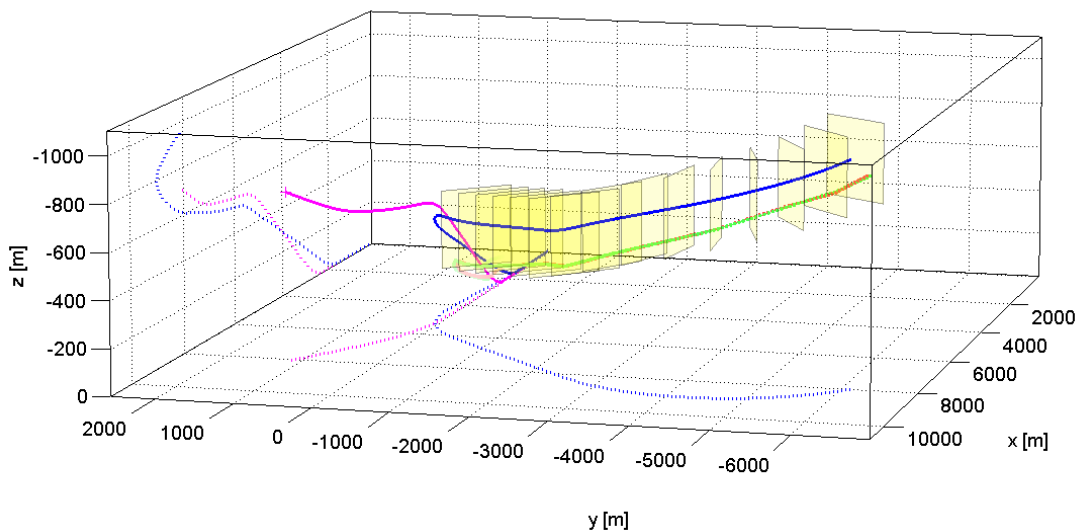


**Figure 3.** Perspective view of trajectories of wake-generating aircraft (blue) and follower aircraft (magenta) together with wake vortex positions (starboard vortex green, port vortex red). Projections of aircraft trajectories on vertical and horizontal planes and a number of gates used for wake vortex prediction are displayed for convenience.

NOWVIV has previously been successfully employed for predictions of wake vortex environmental parameters in five field campaigns (Holzäpfel et al. 2009). The one-year meteorological data base has been validated against a 30-year wind climatology and a 40-days subset has been compared to ultrasonic anemometer, SODAR/RASS, and lidar measurement data (Frech et al. 2007). Assessments of wake prediction skill based on predictions of meteorological conditions with NOWVIV can be found in Frech & Holzäpfel (2008) and Holzäpfel & Robins (2004).

The data base consists of about  $1.3 \cdot 10^6$  vertical profiles of meteorological data at locations separated by one nautical mile and an output frequency of 10 minutes. The meteorological quantities comprise the three wind components, air density, virtual potential temperature, turbulent kinetic energy, eddy dissipation rate (EDR), and pressure.

### Trajectory Model

The risk to encounter a wake vortex is strongly correlated with the actual flight paths of the vortex generating aircraft and the encountering aircraft in space and time. Aircraft trajectories are modeled beginning on runway 25R along five different standard departure routes until 3000 ft above ground (see Figure 2). A large number of environmental and aircraft specific parameters influence an aircraft trajectory. The trajectory model (see Amelsberg & Luckner, 2007 for details) simulates the impact of the most relevant parameters that are: the selected runway and the standard departure route; meteorological condi-



tions including air temperature, density, pressure, wind direction and strength; aircraft type; aircraft take-off weight; takeoff thrust that can be either takeoff go around (TOGA) thrust, or flex takeoff thrust (reduced thrust); start position on the runway; and pilot behavior that is described as a control model considering delayed pilot reaction time and a cross track error.

These factors are varied within defined boundaries and given probability distributions employing Monte Carlo Simulation to generate a set of trajectories for different aircraft types and departure conditions. The aircraft trajectory is adequately described with the equations of motion for three translational degrees of freedom. A deterministic verification has been accomplished by comparing results of the trajectory model with high-fidelity simulation data of departures that were simulated on the certified A330-300 full-flight simulator (A330-FFS) at TU Berlin. Furthermore, a statistical validation was performed by comparing Monte Carlo Simulation results of the trajectory model with 20,000 measured departures at Frankfurt airport provided by DFS Deutsche Flugsicherung GmbH.

Figure 4 shows exemplarily results of 1000 simulated A320 departures. The simulations are based on variations of pilot behavior, aircraft weight, thrust mode and wind conditions. In Figure 4 the resulting mean trajectory and its standard deviations (blue) are compared to the respective measurement data (red). The agreement of the lateral flight path, the climb profile, and the speed profile is sound.

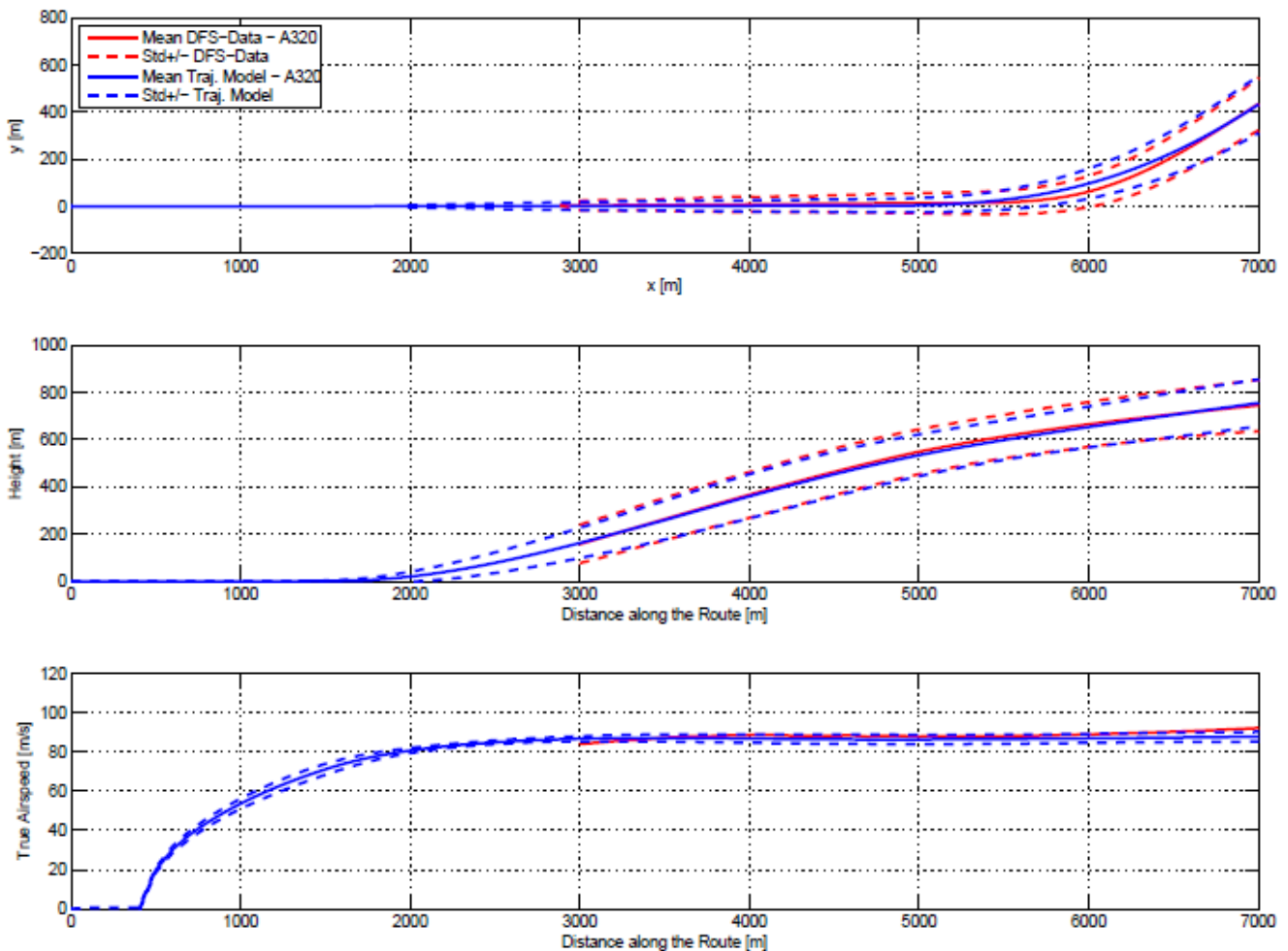


**Figure 4.** Statistics of 1000 departures of A320 aircraft. Lateral and vertical positions and speed profile.

### Wake-Vortex Prediction Models

In the CREDOS project WakeScene provided a choice between two different parametric wake-vortex prediction models. These are the Deterministic Two-Phase wake-vortex decay model (D2P) and the Deterministic wake Vortex Model (DVM). Both vortex models have been validated for departing aircraft by evaluating statistics of the deviations between measured and predicted wake vortex behavior employing data acquired during the two CREDOS field measurement campaigns at Frankfurt airport. The alternative application of two wake vortex models allows assessing the sensitivity of WakeScene-D results on wake vortex parameterizations.

A few adaptations were necessary to comply with the architecture devised for WakeScene-D. The control gates in which the vortices evolve (see Figure 3) are inclined by the flight path angle  $\gamma$  with respect to the vertical direction. For curved flight the vortices are initialized in positions rotated by the bank angle  $\Phi$  such that the vortices descend in a direction tilted by  $\Phi$ . The wake vortex transport by headwind or tailwind is modeled by the respective transport of the gates. Because the gates have arbitrary orientations and move through the space, the determination of the closest distance between wake vortex and follower aircraft requires somewhat complex calculations.

The probabilistic vortex model P2P, which constitutes the basis of its deterministic version D2P, is described in detail in Holzäpfel (2003). Applications, assessments and further developments are reported in Frech & Holzäpfel 2008, Holzäpfel & Robins 2004, Holzäpfel 2006, and Holzäpfel & Steen 2007. In total, P2P has been validated against data of over 10,000 cases gathered in two US and six European measurement campaigns. D2P accounts for the effects of wind, axial- and crosswind shear, turbulence, stable thermal stratification, and ground proximity. Figure 5 delineates a comparison between measured wake vortex positions and circulation and the predictions of the two wake vortex models. Note the effective lateral transport of the vortices in a case with a crosswind of about 4 m/s. Further output provided to VESA includes vortex core radii and the interception angles between aircraft flight path and vortex axis, the so-called encounter angles.

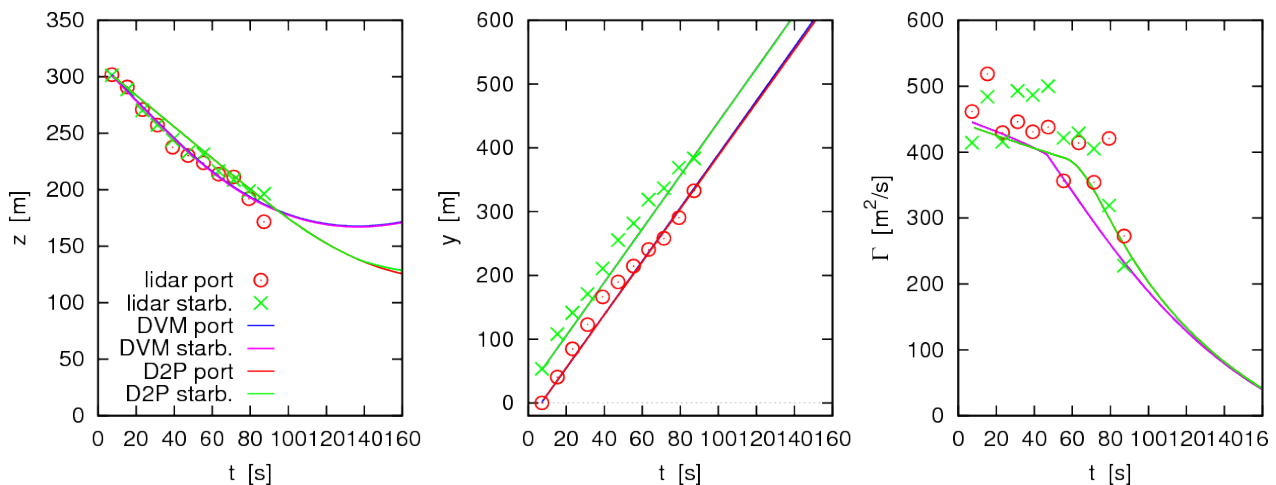


**Figure 5.** Example for evolution of vertical and lateral positions and circulation in a case with a crosswind of about 4 m/s from CREDOS EDDF-1 campaign. Measurements by lidar (symbols) and predictions with D2P and DVM wake vortex models (lines).

The Deterministic wake Vortex Model (DVM) is the new wake vortex predictor software developed by UCL, establishing a step forward in terms of robustness, modularity and performance. It is based on the numerical methodology and the physical models of the Vortex Forecast System (VFS), originally developed by an international (Jackson et al. 2001) and further improved and calibrated (against two US and two EU campaigns, and against LES) since 2002 in the framework of various EU-funded projects. The



DVM accounts for the effects of wind transport (cross and axial), wind shear, decay due to turbulence, stratification, and ground proximity (Winckelmans et al. 2005). It also includes improvements regarding the evaluation of the vertical profiles of environmental conditions and of the In-Ground-Effect model. The Probabilistic wake Vortex Model (PVM) is using the DVM in a Monte Carlo approach, taking into account the uncertainties and variations of the impact parameters from the aircraft and meteorological side and of some physical model coefficients of the DVM.

### Hazard-Area Module

The Hazard-Area Module computes the distance of the follower aircraft (center of gravity) to the vortex centers within each gate along the flight path. Then the closest distance between the follower aircraft and the vortex pair over all gates along the flight path is determined by interpolating aircraft trajectories and wake trajectories between the gates. This closest approach is used for further statistical analysis with WakeScene-D (e.g. vortex age and circulation for this point in time).

In order to estimate the severity of the potential wake vortex encounter an Area of Interest can optionally be defined around the vortices. If the trailing aircraft penetrates this Area of Interest the wake vortex encounter is classified as potentially hazardous. This is considered as a preliminary severity assessment. A corresponding concept called Simplified Hazard Areas has been developed in Schwarz & Hahn (2006) and adapted for take-off and departure. Cases violating the Area of Interest can be subject to more detailed severity assessment with VESA.

### Estimation of Uncertainty

Any software which may be employed to assess the safety of a wake-vortex advisory system must constitute a sufficiently accurate representation of the projected operation. However, for complex risk assessment tools straightforward validation appears not feasible, because the significant manifold of modeled parameters can not be measured simultaneously and reconstructed consistently in a simulation. For WakeScene-D the identification of the relevant processes and the definition of the appropriate degree of details with which they have to be modeled rely on thorough discussion and expert opinion. For the validation of the employed sub-models we refer to the studies cited above.

Here we perform exemplarily a simple estimation of uncertainty for the most important parameter, which is lateral vortex transport, at a vortex generator height of about 50 m, which is within the most critical height range of 100 m above ground (Elsenaar et al. 2006). For B744 and A343 aircraft the difference of predicted and measured standard deviations of lateral aircraft position amounts to  $\sigma_{ac} = 6.8$  m. For these aircraft types the median RMS deviation of measured and predicted wake vortex positions employing the D2P model has been estimated to  $\sigma_{vort} = 19.2$  m (Holzäpfel & Steen 2007). For our purposes here the statistics only need to be accurate on average; i.e. the predictions do not need to be correct in space *and* time. Because the vortex position uncertainty is dominated by spatial and temporal variations between the measured crosswind and the crosswind sensed by the vortices the latter estimation is outmost conservative. Therefore, it can be understood that the vortex prediction uncertainty also implies uncertainties from numerical weather prediction. Assuming that these uncertainties are independent and statistically stationary, the overall uncertainty amounts to  $\sigma_{tot} = (\sigma_{ac}^2 + \sigma_{vort}^2)^{1/2} = 20.3$  m. For this scenario and 120 s old vortices WakeScene-D determines a vortex spreading with  $\sigma_{obs} = 337.3$  m. Hence, a very conservative estimation of the relative uncertainty of lateral vortex positions in ground proximity can be estimated to 6.0.

### Reference Scenario

The described scenario serves as a reference which shall represent the real current departure situation. The working hypothesis assumes that the encounter frequencies estimated for reduced separations under appropriate crosswind conditions shall not be higher than in the reference scenario. Note that the encounter frequencies denote the fraction of encounters within a given scenario. In order to obtain the

absolute probability of encounters in a scenario, the encounter frequency must be multiplied by the frequency of the considered crosswind situation.

The reference scenario employs a sample size of 1,000,000 aircraft pairings. A306, A310, A333, A343, B744 and B772 aircraft are used as vortex generators and A320, AT45, B733 and CRJ as followers. The traffic mix is modeled according to the statistics of Frankfurt airport in 2006 (Anon. 2006). All follower aircraft obey the 120 s ICAO separation. The following parameters of the generator and the follower aircraft are randomly distributed: start point, take-off weight, thrust mode (TOGA take off go around or FLEX take off (reduced) thrust), departure route combination, trajectory deviation, and pilot delay parameter. We employ randomly chosen meteorological data of the NOWVIV one-year data base within the operational hours of Frankfurt airport (6:00 – 23:00). Furthermore, cases with tailwinds above 5 knots are excluded. The constraints regarding operational hours and tailwind are also applied for all other investigated cases.

Figure 6 singles out the fraction of departures (70,167 cases or 7.0%) in which the follower aircraft approach the vortices closer than 50 m and the vortices still have at least a circulation of 100 m<sup>2</sup>/s. These cases potentially correspond to an encounter and should be understood as cases of interest or potential encounters. Detailed investigations with VESA are necessary to identify the risks related to such potential encounters. For convenience we call these cases simply encounters without regard to the real connected risks.

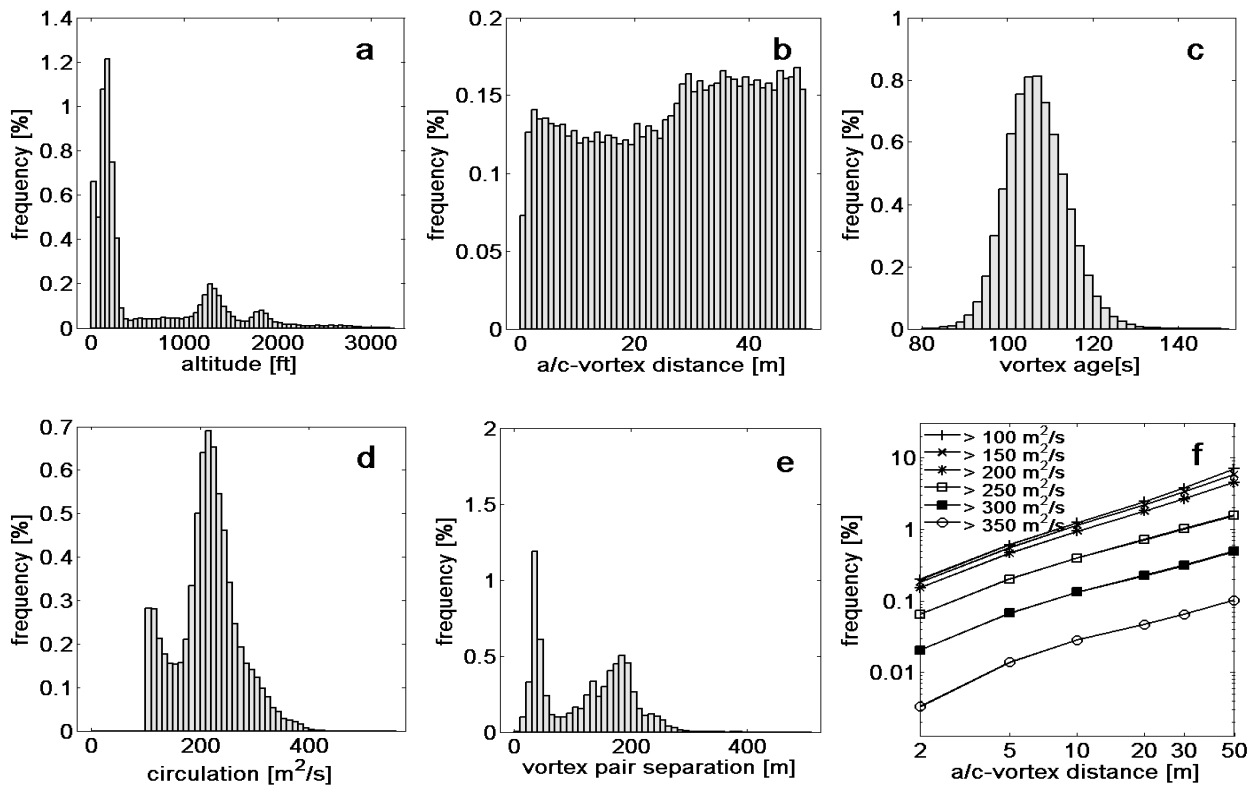
Remarkably, 66% of these “encounters” are restricted to heights below 300 ft above ground (see Figure 6a). Within this altitude range clearance of the flight corridor by descent and advection of the vortices is restricted: stalling or rebounding vortices may not clear the flight path vertically and weak crosswinds may be compensated by vortex-induced lateral transport (Holzäpfel & Steen 2007). This culmination of vortex encounters at low altitudes indicates that the sought crosswind criterion could be limited to this height range, which would substantially facilitate the implementation of an operational system.

Further, minor peaks at 1300 ft and at 1800 ft occur in Figure 6a. These minor peaks can be attributed to flight path changes which increase the encounter risk compared to approximately parallel flight of the leader and follower aircraft. Figure 7 exemplifies a typical situation: At about 1500 ft the leading aircraft reduces thrust and thus the climb rate; at the same time it initiates a turn towards a southerly direction. The combination of this flight path diversion with a strong headwind component which counteracts the vortex descent and a southerly wind direction leads to the displayed encounter at 1250 ft. The second cluster of encounters at 1800 ft is related to the resumption of climb when the aircraft reach the final climb speed. A number of other combinations of flight path diversions and adverse wind directions have been identified, both for identical and different departure routes of the leader and follower aircraft.

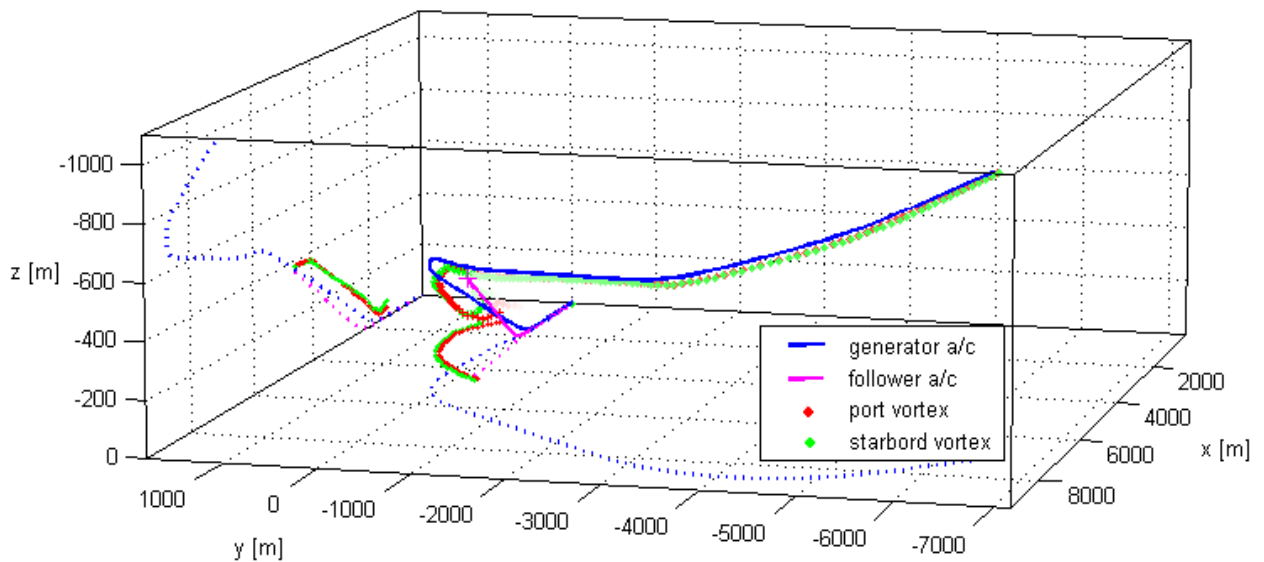
Figure 6b reveals that within the 50 m distance the encounter frequency depends only weakly on the separation between aircraft and wake vortices. Figure 6c and d indicate a considerable range of vortex ages between 80 s and 150 s corresponding to vortex strengths between 100 and 430 m<sup>2</sup>/s. The irregular circulation distribution in Figure 6d is mostly related to differing vortex decay characteristics of the different generator aircraft types in combination with different decay rates in ground proximity and aloft. Figure 6e illustrates that in 19% of the encounters the vortices still approximately retain their initial vortex spacings ranging from 34.5 m to 50.6 m for the selected vortex generator aircraft types. The cluster of vortex separations beyond 100 m represents the range typically occurring after vortex rebound in ground proximity.

Figure 6f displays encounter frequencies dependent on the minimum distance between the follower aircraft and the vortex during the whole departure and the respective circulation,  $\Gamma$ . The frequency of encounters with  $\Gamma > 100$  m<sup>2</sup>/s reduces from 7.0% for vortex distances below 50 m to 0.20% for distances below 2 m. For circulations stronger than 350 m<sup>2</sup>/s the encounter frequencies are 0.10% for vortex distances below 50 m and reduce to 0.0037% (37 cases of 1,000,000 departures) for distances below 2 m.





**Figure 6.** Statistics of cases of interest in the reference scenario. a) Aircraft altitude, b) distance between follower aircraft and wake vortex, c) vortex age, d) vortex circulation, e) vortex pair separation, and f) encounter frequencies dependent on distance to the vortex and circulation.



**Figure 7.** Perspective view of trajectories of wake-generating aircraft (blue) and follower aircraft (magenta) together with wake vortex positions (starboard vortex green, port vortex red). Projections of aircraft and vortex positions on vertical and horizontal planes are added for convenience.

The considered range of distances to the vortex and circulation strengths was chosen such that, on one hand, no cases of interest are missed and, on the other hand, the rarest strong encounters are captured. Note that the weakest potential encounters ( $\Gamma > 100 \text{ m}^2/\text{s}$ , aircraft-vortex distance  $< 50 \text{ m}$ ) in many cas-

es may not lead to any perceptible interference. On the other hand, close encounters on the order of 2 m to 5 m are almost not feasible because they are impeded by wake vortex induced aircraft reactions. In this approach factors like encounter angles, flight attitude and altitude of the follower aircraft are neglected. Therefore, only VESA which fully considers the encounter situation including the interaction of aircraft and wake vortex may really evaluate the related risks. Because VESA investigations are out of the scope of this paper, the metrics of Figure 6f are used to relatively compare the risks of the different scenarios. A target scenario is considered safe when all these joint frequencies are below the reference scenario.

### Crosswind Dependency

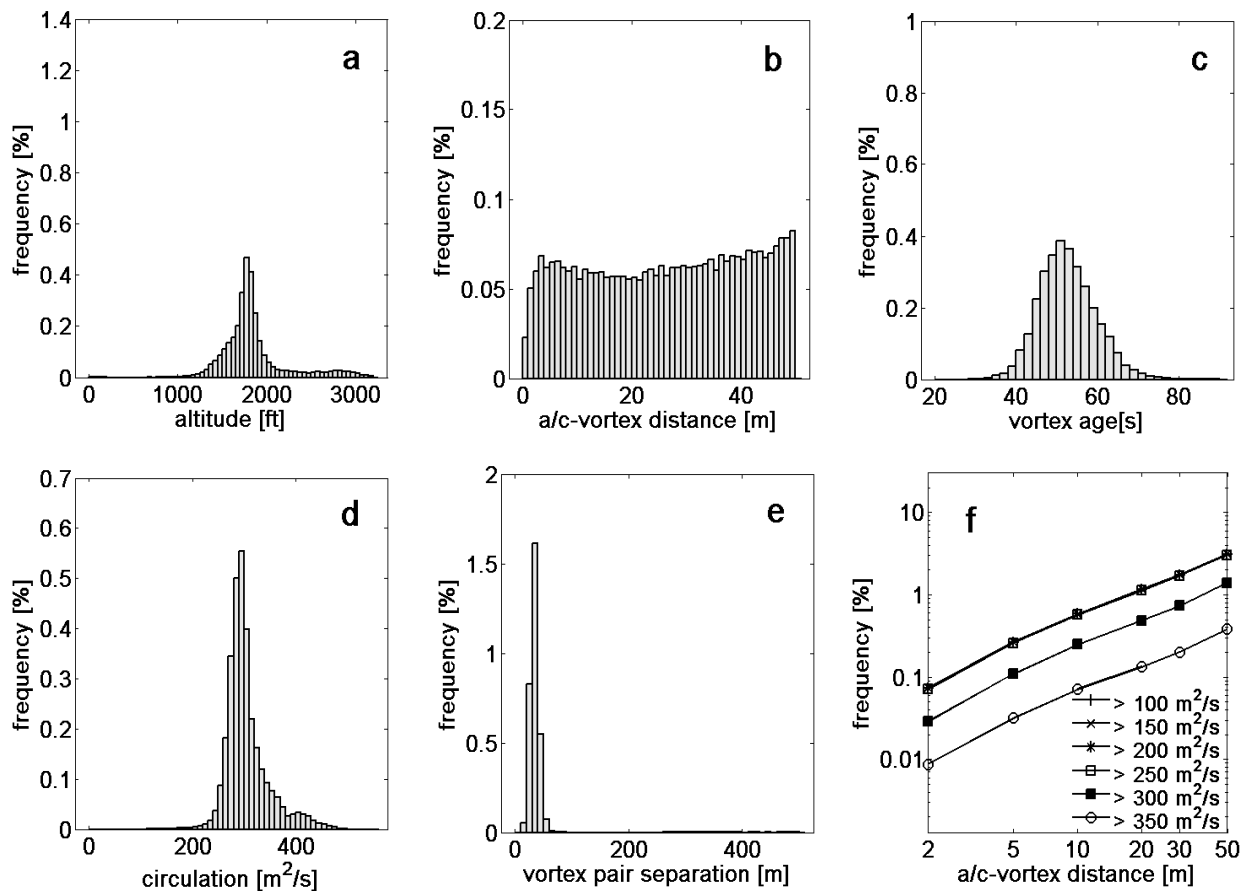
Statistics of encounter frequencies and encounter conditions have been produced for 60 s and 90 s departure separations and crosswind thresholds from 0 to 10 knots in 2 knot increments, respectively. All other parameters correspond to the reference scenario. The crosswind criterion is met when the crosswind at 10 m height above ground exceeds a predefined threshold. This crosswind criterion has been selected because (i) 10 m is the standard height for surface wind measurements and thus constitutes the operationally simplest approach for crosswind dependent reduced separations. (ii) Most encounters are restricted to heights below 300 ft above ground. (iii) An investigation of wind conditions at Frankfurt airport (Dengler & Wiegele 2008) reports a 95%-correlation of the crosswind at 100 m height with the 10 m wind measurement.

Three independent analyses of field measurement data of wake vortices generated by departing aircraft in an altitude range from 0 to 400 m at Frankfurt airport have been performed within the CREDOS project to determine crosswind thresholds which ensure that the wake vortices have left a safety corridor at certain aircraft separation times (Dengler et al. 2011). Although the three analyses employ different assumptions on the safety corridor definition and size, the employed confidence levels, and the crosswind measurement sources and definitions, they consistently yield crosswind thresholds on the order of 4 m/s to make sure that the wake vortices have escaped a safety corridor at a vortex age of 60 s with a high probability based on good quality wind measurements. Note that such studies do not allow quantifying the related risks and setting the risks into relation to the current ICAO operations.

The corresponding WakeScene-D results for aircraft separations of 60 s and crosswinds above 8 knots (4.1 m/s) are displayed in Figure 8. The overall frequency of encounters of 3.1% (31,239 cases) is clearly below the corresponding frequency of 7.0% of the reference scenario. Figure 8 shows in agreement with the experimental results that the strong crosswind in ground proximity is outmost effective. The remaining 56 encounters below 300 ft can be almost neglected compared to the corresponding 45,962 encounters in the reference scenario. Now the peak at 1800 ft related to flight path diversions clearly dominates the scenario.

The encounter synopsis in Figure 8f indicates that despite of the reduction of the overall encounter frequencies the encounters with circulations stronger than  $350 \text{ m}^2/\text{s}$  are still 2 to 4 times more frequent than in the reference scenario in Figure 6f. This can be explained by the halved time for vortex decay. Two facts may potentially reduce the hazard of the current encounters compared to the reference scenario. The encounters occur at sufficiently high altitudes to provide ample time for pilots to recover. The encounter angles are increased which could potentially reduce adverse effects for the follower aircraft.

**Figure 9.** Figures 9 and 10 depict the so-called encounter angles  $\gamma$  and  $\psi$  which denote the inclination angle and the azimuth angle between vortex axis and flight path of the follower aircraft, respectively. Negative inclination angles  $\gamma$  denote situations where the aircraft approach the vortex from below. Negative azimuth angles  $\psi$  refer to encounters from the left, i.e. the aircraft hit in general the port vortex.



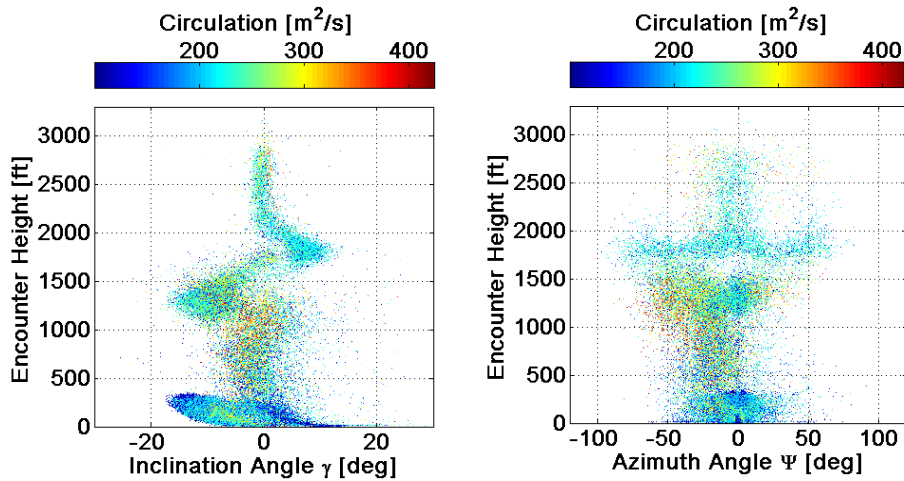
**Figure 8.** Statistics of cases of interest for aircraft separated by 60 s and a crosswind threshold of 8 kn.

Figure 9 shows the encounter angles with color-coded circulation values for the reference scenario. The predominantly negative inclination angles  $\gamma$  below 300 ft correspond to cases where the aircraft approach the wake vortices from below after the vortex rebound. Due to the ground induced decay the corresponding circulation values are relatively low. Aloft the inclination angles on average are slightly negative. This can be explained to some extent by the steeper climb rates of the follower aircraft and to some extent by reduced descent rates of aged wake vortices. At about 1500 ft the aircraft reduce the climb rate in order to accelerate. Below that altitude range the aircraft with higher climb rates encounter less inclined vortices ( $\gamma < 0$ , see Figure ). Inversely, positive inclination angles (encounter from above) occur in the altitude range where the follower aircraft with lower climb rates encounter wake vortices which were generated by aircraft which have already resumed climb when they have reached the final climb speed.

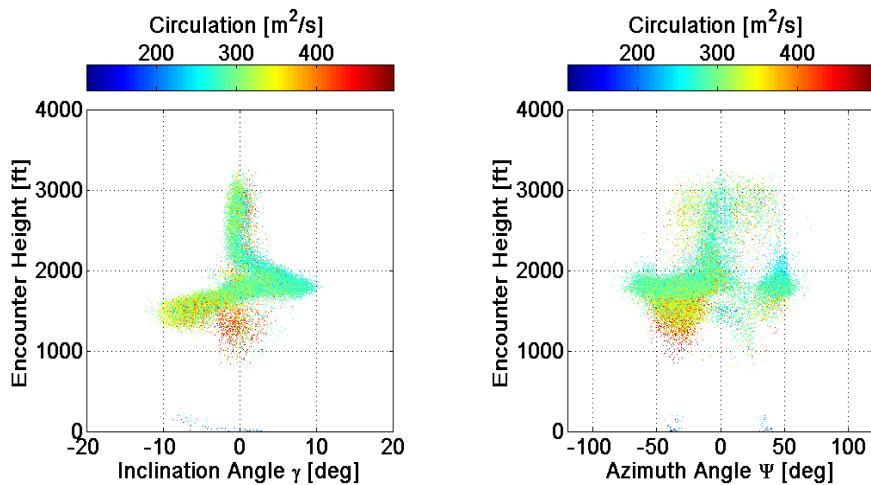
The azimuth angles  $\psi$  are on average negative. This can probably be attributed to the more frequent south-westerly winds. Crosswinds directed from port to starboard are tilting the vortices in azimuthal direction because the longer residence times of older vortex segments lead to larger transport distances. The turns around 1500 ft and 2000 ft (see Figure 2) lead to increased encounter azimuth angles with either sign depending on the departure route combinations and the wind direction (see Figure 7).

Figure 10 shows the encounter angles for 60 s aircraft separations with crosswinds above 8 knots. Now encounters at low altitudes have almost completely disappeared. Most of the remaining encounters are occurring above 1000 ft and can be explained by the flight path changes discussed above. A remarkable concentration of encounters with strong vortices between 1000 ft and 1700 ft occurs with inclination angles centered on zero and azimuthal angles around 30 deg. These strong encounters mainly occur if

the leading aircraft follows a southerly departure route. In these cases the leading aircraft have already initiated a turn without reducing the climb rate and south-westerly winds compensate vortex induced descent.



**Figure 9.** Encounter angles  $\gamma$  (inclination angle) and  $\psi$  (azimuth angle) dependent on altitude with color-coded circulation for the reference scenario.



**Figure 10.** Encounter angles dependent on altitude with color-coded circulation for 60 s aircraft separations with crosswinds above 8 knots.

Table 1 provides a synopsis of the encounter frequencies for the investigated crosswind and departure separation scenarios. The crosswind threshold and aircraft separation combinations where the encounter frequencies fall below the reference scenario (highlighted in dark grey) are highlighted in light grey. In summary crosswinds are very effective to reduce encounter frequencies close to the ground already for crosswinds stronger than 4 knots (6 knots) at 90 s (60 s) aircraft separations. As a consequence, the encounters at higher altitudes become more prominent. Due to the reduced time for vortex decay worst case encounter frequencies aloft are not reduced very effectively by increasing crosswinds.

Figure 11 shows the frequencies of the crosswinds in the meteorological data base in 0.5 knot increments (All CWs) and the respective encounter frequencies versus crosswind speed for aircraft separations of 60 s, 90 s, and 120 s. The left plot displays absolute frequencies whereas the relative frequencies shown on the right are normalized to 100%. Figure 11 indicates that the highest encounter frequencies are not observed for zero crosswinds. For the reference scenario 120 s and the 90 s departure separations they occur instead around crosswinds of  $\pm 1$  to  $\pm 1.5$  knots. If the aircraft separation is re-



duced to 60 s, the most critical crosswinds amount to  $\pm 2.5$  knots. This is due to the fact that weak crosswinds may compensate the vortex-induced lateral propagation speed of wake vortices generated in ground proximity such that the luff vortex is hovering above the runway (Holzäpfel & Steen 2007). For the 60 s separation the critical crosswind magnitude is higher because the crosswind has less time to transport the vortices out of the flight corridor.

**Table 1.** Synopsis of encounter frequencies for different aircraft separations and crosswind scenarios.

Scenario	120 s	90 s	90 s	90 s	90 s	90 s	90 s
	all CWs	60 s all CWs	60 s CW > 2kts	60 s CW > 4kts	60 s CW > 6kts	60 s CW > 8kts	60 s CW > 10kts
total encounter frequency	7.0%	12.8%	7.5%	3.7%	2.6%	2.2%	1.9%
encounter frequency below 300 ft	4.6%	9.4%	2.9%	0.057%	0.0003%	0.0002%	0.0%
worst case encounter frequency	0.0037%	0.023%	0.011%	0.0073%	0.0041%	0.0026%	0.0017%
		0.11%	0.056%	0.020%	0.010%	0.0086%	0.0025%

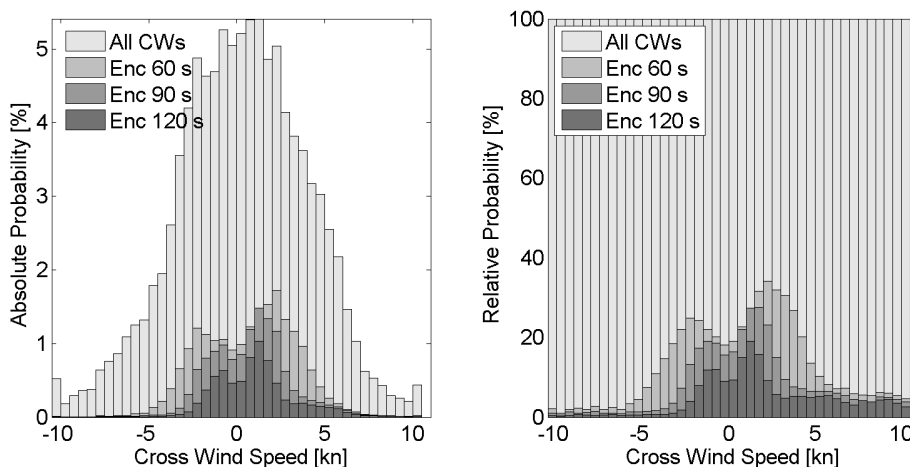


**Figure 11.** Left: Crosswind distribution in 0.5 knot increments and respective absolute encounter frequencies for different aircraft separations. Relative encounter frequencies right. Winds blowing from the port side are positive.

Figure 11 right indicates that for the 120 s separation crosswinds above 2.5 knots do not significantly reduce the relative encounter frequencies. For the 90 s separation this is the case above about 4 knots and for the 60 s separation the corresponding threshold is at about 6 knots. Beyond these thresholds the encounters at high altitudes related to flight path diversions constitute the dominant risks.

Somewhat surprisingly the histograms are not symmetric. Note that already at -5 to -5.5 knots the relative encounter frequency for 60 s separations is lower than the encounter frequency for 5 to 5.5 knots for the 120 s reference scenario. Several reasons for the asymmetry can be identified: (i) the realistic meteorological data base contains distributions of wind speed and direction which are not only the result of predominant synoptic patterns but are also influenced by the orography in the vicinity of the airport, in

particular the Taunus mountain ridge. (ii) The winds aloft generally deviate from the winds at 10 m altitude and (iii) the departure routes are not symmetric with respect to the runway. (iv) The most important and fundamental effect, however, is related to the turning of the wind direction to the right with increasing height (Ekman Spiral). This effect is described in more detail below.

### Comparison to Field Measurement Data

The validation activities for the individual sub-models and data bases of WakeScene-D and an estimation of the related uncertainties are described above. Here we perform a *global* comparison of wake vortex transport characteristics achieved with long-term measurements and WakeScene-D simulations. Note that this comparison assumes that the employed data sample is sufficiently large to provide converged wake vortex transport statistics in a climatological sense. During the six months CREDOS measurement campaign EDDF-2, vortex tracks of about 10,000 departures from runway 25R of Frankfurt airport were collected with the WindTracer lidar (Dengler & Wiegele 2011). The lidar measurement plane was situated 2961 m from the threshold of runway 25R (see Figure 2) where 99% of the vortices were measured at heights below 135 m. Wake vortices that might have been advected from runway 25L to 25R are not part of the data set.

To mimic the lidar measurements with WakeScene-D we have simulated 10,000 departures with randomly chosen aircraft types and meteorological data. Wake vortex predictions are interpolated within the lidar measurement plane. The lidar scan pattern leads to vortex observations roughly each 8 s. To provide similar visual impressions of the scatter plots the WakeScene-D wake vortex data are also plotted each 8 s where the instant for the first data point is varied randomly.

Figure 12 shows scatterplots of lateral positions of the port vortex against time based on the lidar measurements and WakeScene-D simulations. Additionally, the medians and distributions for one to three standard deviations are plotted. The comparison of the measurements (left) to the simulated lidar data (center) indicates that the domain covered by the lidar constitutes a sub-domain of the real wake vortex transport distances. Zooming the WakeScene-D simulation data on the area covered by the lidar (right) reveals an excellent agreement between measured and simulated lateral vortex transport characteristics. The main differences are related to shorter lidar observation times caused by a loss of the coherent vortex structure during the decay. This good agreement indicates that WakeScene-D supports investigating realistic wake vortex behaviour in domains and height ranges that are far out of reach of measurements. Because the modelling of wake vortex transport in ground proximity is quite complex it could be assumed that the agreement with observations would be even better at higher altitudes.

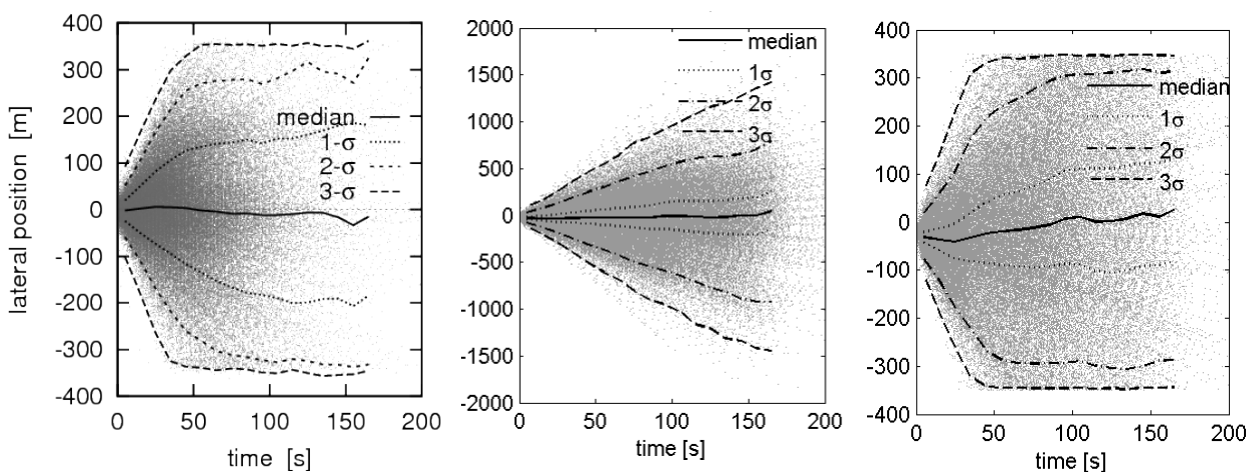


**Figure 12.** Scatterplots and statistical distributions of lateral positions of the port vortices against time for 10,000 departures. Field measurement data (left) and WakeScene-D predictions within different domains (center and right).



## Sensitivity Studies





Comprehensive sensitivity analyses regarding the impact of various sub-models and parameter selections have been performed. A detailed description of all the studies is available in Holzäpfel & Kladetzke (2009).

### Wind Directions

Now effects of wind directions on the encounter frequencies are considered. Four different wind direction sectors are distinguished: headwind, tailwind, crosswind from port side, and crosswind from starboard side. Here the wind directions are defined with respect to the runway direction. So headwinds are blowing from  $315^\circ < \text{RWA} < 45^\circ$  where RWA denotes the relative wind angle with respect to the runway direction. Winds from the starboard side correspond to the wind direction range  $45^\circ < \text{RWA} < 135^\circ$ .

Table 2 lists the encounter frequencies dependent on the four different wind direction sectors for the reference scenario. Headwind situations lead to the highest encounter probabilities because headwind transport of the wake vortices may compensate wake vortex descent or even lead to rising wake vortices with respect to the generator aircraft trajectory. This effect increases encounter frequencies because the medium weight class followers usually take off earlier than the leader and climb steeper than the leading aircraft and therefore usually fly above the wake vortices. In contrast, the encounter frequencies for tailwind situations are much lower (more than a factor of five), because tailwinds support wake vortex descent.

**Table 2.** Encounter frequencies dependent on four different  $90^\circ$  wind direction sectors for the reference scenario. The wind sector icons assume a flight direction from right to left.

SID-comb. wind dir.	all	N-N (16.0 %)	N-S (24.0 %)	S-N (24.0 %)	S-S (36.0 %)
CW port (20.9 %) 	5.2%	4.6%	4.3%	5.3%	6.1%
CW starb. (18.9 %) 	1.7%	1.6%	1.6%	1.5%	1.9%
tailwind (22.4 %) 	2.5%	2.3%	2.1%	2.4%	2.9%
headwind (37.8 %) 	13.3%	13.4%	13.3%	13.0%	13.4%

However, the smallest encounter frequencies are observed for crosswinds from the starboard side. Here the crosswinds close to the ground reduce encounter frequencies. With increasing height the wind direction turns on average to the right. Consequentially, a tailwind component is added to the crosswind which supports vortex descent and thus reduces encounter frequencies aloft.

The turning of the wind direction with altitude is related to the concept of the Ekman spiral depicted in Figure 13: Above the atmospheric boundary layer with a thickness on the order of 1 km the wind direction is mainly controlled by the equilibrium of the driving pressure gradient force and the Coriolis force. The resulting wind is called geostrophic wind. In the atmospheric boundary layer the friction force causes a deviation of the wind direction to the left (on the northern hemisphere).

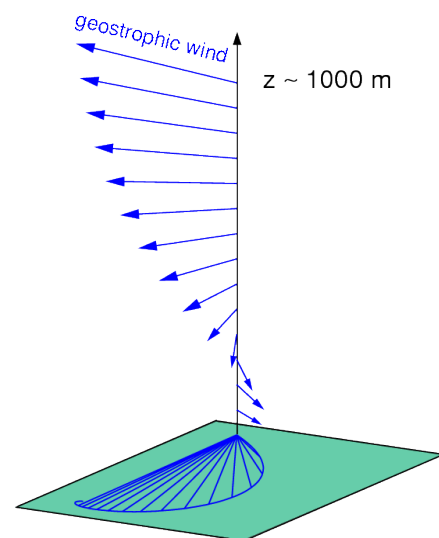






**Fig. 13.** Schematic sketch of Ekman spiral.

Due to the same mechanism crosswinds from port side receive a headwind component with increasing height. As a consequence, the port crosswind situation leads to three times more encounters than the starboard side crosswinds. Additionally, crosswinds from the port side also support encounters for departures of the leading aircraft on the southerly departure routes. There is also some weak trend that the strongest circulation values occur for the headwind encounters (not shown).

Table 3 lists the wind direction effects for 60 s aircraft separations and crosswinds above 6 knots. Because cases with tailwinds above 5 knots are excluded from operations, the wind sector for tailwinds has no contributions. The encounter frequencies for headwinds and for crosswinds from the port side are now almost identical. Considerable differences occur between the different departure route combinations. Small encounter frequencies are observed for headwinds and crosswinds from the port side (southerly winds) for leading aircraft on the northern departure routes and, conversely, for crosswinds from the starboard (northerly winds) side for leading aircraft on the southern departure routes. Hence, encounters can be avoided if the crosswind after the turn transports the vortices away from the former flight track, i.e. southerly crosswinds are favorable for turns to the north.

The smallest encounter frequencies occur for crosswinds from the starboard side combined with the S-N SID combination. Here two favorable effects are combined: the turning of the crosswind to a tailwind at increasing altitudes and the fact that the vortex generating aircraft uses the downwind departure route. Crosswinds above 8 knots show similar characteristics with further reduced encounter frequencies.

**Table 3.** Encounter frequencies and corresponding circulation strengths dependent on four different 90° wind direction sectors for 60 s aircraft separations and crosswinds above 6 knots.

SID-comb. wind dir.	all	N-N (16.0 %)	N-S (24.0 %)	S-N (24.0 %)	S-S (36.0 %)
CW port (38.0 %) 	5.5%	1.8%	1.4%	7.7%	8.5%
CW starb. (44.7 %) 	1.5%	0.9%	3.5%	0.2%	1.3%
tailwind (0 %) 	–	–	–	–	–
headwind (17.2 %) 	5.8%	1.6%	2.7%	7.9%	8.3%

### Key Results of Remaining Studies

**Sample size:** It must be guaranteed that the sample size of the Monte Carlo simulations is sufficiently large to provide converged simulation results also for rare events. For this purpose statistics of encounter frequencies derived from sample sizes of  $10^4$ ,  $5 \cdot 10^4$ ,  $10^5$ ,  $2 \cdot 10^5$ ,  $5 \cdot 10^5$ , and  $10^6$  departures of aircraft pairings have been analysed for different scenarios. It was found that a reasonable representation of the frequencies of the most critical and rare encounters requires sample sizes of 500,000 departures of aircraft pairings. Therefore, the one million sample size used for the current investigations guarantees well converged statistics.

**Operation times:** By default the meteorological data of the NOWVIV one-year data base is employed only within the operational hours of Frankfurt airport (06:00 – 23:00). A comparison to 24 h operations indicates a minor increase of encounter frequencies for nocturnal meteorological conditions. This can potentially be explained by the reduced turbulence in the residual layer which increases vortex lifetimes and the increased temperature stratification which reduces vortex descent.





**Flight path adherence:** Deviations from nominal flight tracks in vertical and horizontal direction have been determined being on the order of 100 m. Therefore, the sensitivity of encounter frequencies of the standard flight path deviation model has been compared to a version in which these deviations were deactivated. The study indicates that the deactivation of aircraft trajectory deviations only slightly reduces the encounter frequencies.

**Pull-away effect:** In contrast to arrivals where a close-up effect on average reduces aircraft separations, an increase of average aircraft separations is expected for departures. The reason is that at a given time the leading aircraft has arrived in general already at a higher flight speed than the follower aircraft. The simulations indicate that the separation increases are spread between 0 to 3 NM that is the minimum initial separation is never reduced. The pull-away effect is the more pronounced the more the initial aircraft separations are reduced.

**Departure Routes:** For the encounter statistics with crosswinds above 8 knots the differences between the departure route combinations are quite prominent because the encounters in ground proximity (which are independent from SID combinations) are already quite rare (see Figure 8) and many encounters aloft are related to flight path diversions. As a result for a generic airport the SID combination study indicates that reduced departure separations could be supported by crosswinds above 8 knots for a straight departure route. For diverging departure route combinations the procedure could be refined by using only SID combinations where the leading aircraft is flying on the downwind SID.

**Wake vortex model:** Wake vortex modeling constitutes a very important element of WakeScene-D. Therefore, the statistics achieved with the D2P wake vortex model have been compared to results of the Deterministic Vortex Model (DVM). The two wake vortex models deliver very similar characteristics of encounter altitude, the distance between follower aircraft and wake vortex, and vortex age. The circulation distributions exhibit different characteristics but almost identical ranges. In ground proximity the D2P model predicts more pronounced vortex spreading. For the statistics of encounter strength and distance between aircraft and vortex similar characteristics are found. The corresponding deviations are naturally more pronounced for the rare encounters and reside typically within a range of 5% to 30%. Because the encounter frequencies of equal strength vary between the different scenarios by up to almost two orders of magnitude, the agreement between the encounter statistics of the two wake vortex models is considered as good. In particular, the conclusions derived from the synopsis of the encounter frequencies in Table 1 would be identical with the DVM wake vortex predictions.

**Aircraft-type combinations / Take-off weight:** The encounter frequencies of the considered scenarios have been filtered to attribute the encounters to the 24 possible leader/follower combinations. As expected encounters are avoided if the leading aircraft take off late and climb slowly whereas the follower aircraft take off early with a steep climb rate. Thereby, the respective flight tracks are well separated. In contrast, if the leading aircraft take off early and climb steeply whereas the follower aircraft take off relatively late, the resulting flight tracks may be close to each other leading to high encounter probabilities. The same interrelations also apply to the take-off-weight distributions (which correlate with take-off positions and climb rates) within specific aircraft type combinations.

**Comparison to arrival situation:** The comparison of the current reference scenario (see Figure 6f) to WakeScene results for arrivals obeying the ICAO minimum separation of 5 NM between heavy and medium aircraft in (Holzäpfel et al. 2009-1) indicates that encounters ( $\Gamma > 100 \text{ m}^2/\text{s}$  and distances to the vortices below 30 m) are 5.6 times more frequent for arrivals (21.5%) than for departures (3.8%). For approaches the accumulation of encounters within a height range below 300 ft is with about 95% even more pronounced. The reason for these differences can mainly be attributed to the much more pronounced spreading of aircraft trajectories for the departure situation which is caused by e.g. large variations of rotation point and climb rate. Note that the considered departure and arrival scenarios can not be directly compared due to differences regarding sample size and traffic mix. Further, in the arrival simulations the aircraft are already installed on the glide slope whereas for departures waypoints with diverging flight routes are considered.

## Implementation of Lessons Learned

Here we investigate an advanced crosswind scenario which is based on the lessons learned from the sensitivity analysis. First, we restrict the analysis on the northern departure routes used by default at Frankfurt airport where encounters are relatively rare. Second, we differentiate crosswinds blowing from the port side and the starboard side of the departing aircraft. Encounter frequencies for 60 s departure separations and a crosswind threshold of 6 knots indicate that for positive crosswinds (wind from port side) the worst case encounter frequency of 0.0082% is higher than in the reference scenario (see Table 1). However, for crosswinds below -6 knots (wind from starboard side) the encounter frequencies of all circulation and distance thresholds are smaller than in the reference scenario (worst case encounter frequency is 0.0031%). In conclusion, the consideration of the northern departure routes as used routinely at Frankfurt airport yields encounter frequencies below the reference scenario for all considered vortex distances and circulation strengths for crosswinds below -6 knots (wind from starboard side) and for crosswind magnitudes above 8 knots. The assessment of the related encounter risks with VESA leads to the same conclusions (Kauertz 2009, Kauertz et al. 2012).

## Conclusions

WakeScene-D is a software package to determine wake vortex encounter probabilities for departures. The severity of potential encounters identified by WakeScene-D can subsequently be evaluated with VESA (Kauertz et al. 2012). In this paper first the components of WakeScene-D which model traffic mix, aircraft trajectories, meteorological conditions, wake vortex evolution, and potential hazard area are briefly introduced. Then various investigated scenarios are discussed which shall support the identification of suitable crosswind criteria that allow reducing aircraft separations for departures.

Measured vortex tracks of about 10,000 departures from runway 25R of Frankfurt airport are compared with WakeScene-D simulations. For lateral vortex transport, which for crosswind departures constitutes the most important quantity, good agreement between the characteristics of measurement and simulation is achieved. This good agreement indicates that WakeScene-D is an instrument which allows investigating realistic wake vortex behaviour in domains and height ranges that are far out of reach of measurements.

Monte Carlo simulations of the Frankfurt traffic mix with a sample size of 1,000,000 cases indicate that for current operations 66% of the potential encounters are restricted to heights below 300 ft above ground. Within this altitude range clearance of the flight corridor by descent and advection of the vortices is restricted: stalling or rebounding vortices may not clear the flight path vertically and weak crosswinds may be compensated by vortex-induced lateral transport (Holzäpfel & Steen 2007). Further, minor peaks at altitudes of 1300 ft and at 1800 ft occur which can be attributed to flight path diversions (change of climb rate and heading) in combination with adverse wind conditions (headwind and crosswind) which increase the encounter risk compared to approximately parallel flight of the leader and follower aircraft. For example, increased encounter frequencies are observed when the leading aircraft conducts a turn towards the main wind direction. The resulting headwind component may compensate wake vortex descent and may advect the vortex trail into the flight path of the follower aircraft.

Statistics of encounter frequencies and encounter conditions have been established for 60 s and 90 s departure separations and minimum crosswinds from 0 to 10 knots in 2 knot increments, respectively. The reduction of aircraft separations from 120 s to 60 s approximately triples the number of encounters, whereas the fraction of strong encounters increases due to the reduced time for vortex decay. If aircraft separations are reduced to 60 s and crosswinds at 10 m height above ground exceed a threshold of 8 knots, the overall frequency of potential encounters of 3.1% clearly is falling below the corresponding frequency of 7.0% of the reference scenario. The strong crosswind in ground proximity very efficiently reduces the encounters below 300 ft from 4.6% in the reference scenario to 0.0056%. Unfortunately, the 10 m crosswind criterion alone is not sufficient to reduce encounters which are related to flight path diversions along the departure routes. Due to the by 50% reduced time for vortex transport and decay,



encounters with circulations stronger than  $350 \text{ m}^2/\text{s}$  are still 2 to 4 times more frequent than in the reference scenario.

An investigation of wind direction effects on the encounter frequencies reveals an intriguing phenomenon: Headwind situations lead to the highest encounter probabilities because headwind transport of the wake vortices may compensate wake vortex descent or even lead to rising wake vortices with respect to the generator aircraft trajectory. This effect increases encounter frequencies because the medium weight class followers usually take off earlier and climb steeper than the leading aircraft and therefore usually fly above the wake vortices. In contrast, the encounter frequencies for tailwind situations are much lower because tailwinds support wake vortex descent.

However, the beneficial effects of crosswinds are not symmetric. The smallest encounter frequencies are observed for crosswinds from the starboard side. Here the crosswinds close to the ground reduce encounter frequencies. With increasing height the wind direction turns on average to the right. Consequentially, a tailwind component is added to the crosswind which supports relative vortex descent and thus reduces encounter frequencies aloft. This turning of the wind direction with height is related to the concept of the Ekman spiral which describes the resulting wind direction in the atmospheric boundary layer by equilibrium of the driving pressure gradient force, the Coriolis force, and the friction force. Due to the same mechanism crosswinds from port side receive a headwind component with increasing height. As a consequence, the port crosswind situation leads to significantly more encounters than the starboard side crosswinds.

From a WakeScene-D perspective it can be concluded that for 60 s departure separations along the northern departure routes as used routinely at Frankfurt airport acceptable encounter frequencies are found for crosswinds below -6 knots (wind from starboard side) and for crosswind magnitudes above 8 knots. The respective assessment of the related encounter risks with VESA leads to the same conclusions also for straight departure routes (Kauertz 2009, Kauertz et al. 2012). Crosswind departure procedures could be refined by using only departure route combinations where the leading aircraft is flying on the downwind route.

Crosswind transport certainly is the most effective mechanism to clear a flight corridor from wake vortices. However, the applicability of purely crosswind based wake vortex advisory systems covering vertically extended domains is impeded by the veering wind with altitude. As a consequence, either the flight tracks of subsequent aircraft must be separated already at quite low altitudes such that the crosswind does not change significantly within the considered height ranges or the advisory system must also consider vortex descent and/or vortex decay either explicitly or implicitly as in the presented concept.

## Acknowledgement

The financial support from the EU project CREDOS (AST5-CT-2006-030837) is greatly acknowledged. Thanks are addressed to many CREDOS colleagues for numerous discussions and valuable comments. In particular, the contributions from Swantje Amelsberg, Helge Lenz (trajectory model), Carsten Schwarz (hazard area module), and Ivan De Visscher (DVM wake vortex model) are highly acknowledged.

## References

- Amelsberg, S., and Luckner, R., "Parametric Aircraft Trajectory Model for Takeoff and Departure," 1st CEAS European Air and Space Conference, CEAS-2007-273, Berlin, Germany, Sept. 2007, pp. 785-795.
- Anon., „Frankfurt Airport Luftverkehrsstatistik 2006,“ Fraport AG, Frankfurt am Main, Germany, 2007.
- de Bruin, A.C., Speijker, L.J.P., Moet, H., Krag, B., Luckner, R., and Mason, S., "S-Wake – Assessment of Wake Vortex Safety," Publishable Summary Report, National Aerospace Laboratory, NLR-TP-2003-243, Amsterdam, 2003.
- Dengler K., Wiegele A., "EDDF-1 Data Collection Campaign Report," CREDOS, D2-1, 25 Nov. 2008.
- Dengler K., F. Holzäpfel, T. Gerz, A. Wiegele, I. De Visscher, G. Winkelmann, L. Bricteux, H. Fischer, and J. Konopka, Crosswind Thresholds Supporting Wake-Vortex-Free Corridors for Departing Aircraft, Meteorological Applications, 2011, DOI: 10.1002/met.261.

- Elsenaar B. et al., "Wake Vortex Research Needs for Improved Wake Vortex Separation Ruling and Reduced Wake Signatures", Final Report of the Thematik Network 'WakeNet2-Europe', 6th Framework Programme, National Aerospace Laboratory, NLR-CR-2006-171, Amsterdam, Mar. 2006.
- Frech, M., and Holzäpfel, F., "Skill of an Aircraft Wake-Vortex Model Using Weather Prediction and Observation," *Journal of Aircraft*, Vol. 45, No. 2, 2008, pp. 461-470.
- Frech, M., and Zinner, T., "Concept of Wake Vortex Behavior Classes," *Journal of Aircraft*, Vol. 41, No. 3, 2004, pp. 564–570.
- Frech, M., Holzäpfel, F., Tafferner, A., and Gerz, T., "High-Resolution Weather Data Base for the Terminal Area of Frankfurt Airport," *Journal of Applied Meteorology and Climatology*, Vol. 46, No. 11, 2007, pp. 1913-1932.
- Gerz, T., Holzäpfel, F., Bryant, W., Köpp, F., Frech, M., Tafferner, A. and Winkelmanns, G., "Research towards a wake-vortex advisory system for optimal aircraft spacing," *Comptes Rendus Physique*, Vol. 6, No. 4-5, 2005, pp. 501–523.
- Grell, G.A., Emeis, S., Stockwell, W.R., Schoenemeyer, T., Forkel, T., Michalakes, J., Knoche, R., and Seidl, W., "Application of a multiscale, coupled MM5/chemistry model to the complex terrain of the VOTALP valley campaign, *Atmospheric Environment*, Vol. 34, No. 9, 2000, pp. 1435-1453.
- Hallock, J.N., Greene, G.C., and Burnham, D.C., "Wake Vortex Research - A Retrospective Look," *Air Traffic Control Quarterly*, Vol. 6, No. 3, 1998, pp. 161–178.
- Höhne, G., Luckner, R., and Fuhrmann, M., "Critical Wake Vortex Encounter Scenarios," *Aerospace Science and Technology*, Vol. 8, No. 8, 2004, pp. 689-701.
- Holzäpfel, F., "Probabilistic Two-Phase Wake Vortex Decay and Transport Model," *Journal of Aircraft*, Vol. 40, No. 2, 2003, pp. 323-331.
- Holzäpfel, F., "Probabilistic Two-Phase Aircraft Wake-Vortex Model: Further Development and Assessment", *J. Aircraft*, Vol. 43, 700-708, 2006.
- Holzäpfel, F., Frech, M., Gerz, T., Tafferner, A., Hahn, K.-U., Schwarz, C., Joos, H.-D., Korn, B., Lenz, H., Luckner, R., and Höhne, G., "Aircraft Wake Vortex Scenarios Simulation Package - WakeScene," *Aerospace Science and Technology*, Vol. 13, No. 1, 2009, pp. 1-11, doi:10.1016/j.ast.2007.09.008.
- Holzäpfel, F., Kladetzke, J., "Wake vortex encounters during take-off & departure: Sensitivity analysis and worst case search," *CREDOS D3-9*, 5 Nov. 2009.
- Holzäpfel, F., Kladetzke, J., Assessment of Wake Vortex Encounter Probabilities for Crosswind Departure Scenarios, *Journal of Aircraft*, Volume 48, Number 3, May-June 2011, pp. 812-822. DOI 10.2514/1.C000236
- Holzäpfel F., Kladetzke J., Amelsberg S., Lenz H., Schwarz C., De Visscher I., "Aircraft Wake Vortex Scenarios Simulation Package for Takeoff and Departure," *Journal of Aircraft*, Vol. 46, No. 2, 2009, pp. 713–717, also AIAA Paper 2008-8921.
- Holzäpfel, F., and Steen, M., "Aircraft Wake-Vortex Evolution in Ground Proximity: Analysis and Parameterization," *AIAA Journal*, Vol. 45, No. 1, 2007, pp. 218- 227.
- Holzäpfel F., R.E. Robins, "Probabilistic Two-Phase Aircraft Wake-Vortex Model: Application and Assessment", *J. Aircraft*, Vol. 41, 1117-1126, 2004.
- ICAO, Procedures for Air Navigation Services - Air Traffic Management, Doc 4444, ATM/501, 2001.
- Jackson, W., Yaras, M., Harvey, J., Winkelmanns, G., Fournier, G., Belotserkovsky, A., "Wake Vortex Prediction - An Overview," Project Final Report, Transport Canada and its Transportation Development Center, Montréal, Canada, March 2001, <http://www.tc.gc.ca/tdc/summary/13600/13629e.htm>.
- Joos, H.-D., Bals, J., Looye, G., Schnepfer, K., and Varga, A., "A multi-objective optimisation based software environment for control systems design," Proceedings of 2002 IEEE International Conference on Control Applications and International Symposium on Computer Aided Control Systems Design, CCA/CACSD, Glasgow, Scotland, U.K., 2002.
- Kauertz S., "Workpackage 3 Final Report" *CREDOS*, D3-11, 25 Nov. 2009.
- Kauertz S., F. Holzäpfel, J. Kladetzke, "Wake Vortex Encounter Risk Assessment for Crosswind Departures," *Journal of Aircraft*, accepted, 2012, 11 pages.
- Luckner, R., Höhne, G., Fuhrmann, M., "Hazard criteria for wake vortex encounters during approach," *Aerospace Science and Technology*, Vol. 8, No. 8, 2004, pp. 673-687.
- Schwarz, C.W., and Hahn, K.-U., "Full-flight simulator study for wake vortex hazard area investigation," *Aerospace Science and Technology*, Vol. 10, No. 2, 2006, pp. 136-143.
- Speijker, L.J.P., Kos, J., Blom, H.A.P., and van Baren, G.B., "Probabilistic wake vortex safety assessment to evaluate separation distances for ATM operations," 22nd Congress of the International Council of the Aeronautical Sciences, NLR TP 2000 326, Harrogate, United Kingdom, Sept. 2000.
- Speijker, L.J.P., Vidal, A., Barbaresco, F., Frech, M., Barny, H., and Winkelmanns, G., "ATCWake: Integrated Wake Vortex Safety & Capacity System," *Journal of Air Traffic Control*, Vol. 49, No. 1, 2007, pp. 17–32.
- Winkelmanns G., Duquesne T., Treve V., Desenfans O., and Bricteux L., "Summary description of the models used in the Vortex Forecast System (VFS)," Univ. Catholique de Louvain, Louvain-la Neuve, Belgium, Apr. 2005.